Article

Journal of
Nanoscience and Nanotechnology
Vol. 19, 882–887, 2019
www.aspbs.com/jnn

Surface Modification of SiO_2 for Highly Dispersed Pd/SiO_2 Catalyst

Ji Soo Kwon[1,2], Ji Sun Kim[3], Hak Sung Lee[2], and Man Sig Lee[1,*]

[1] Green Material and Processes Group, Korea Institute of Industrial Technology (KITECH), Ulsan 44413, South of Korea
[2] Department of Chemical Engineering, Ulsan University, Ulsan 44310, South of Korea
[3] Department of Chemical and Biological Engineering, The University of British Columbia [UBC], Vancouver, British Columbia, V6T 1Z3, Canada

Surface modification of SiO_2 supports was shown to significantly affect the properties of Pd/SiO_2 catalysts. The surface of SiO_2 can be modified by various pretreatment methods. In this study, the effect of different calcination temperatures on support surface was investigated. Pd supported on pretreated SiO_2 was characterized by H_2 temperature-programmed reduction (TPR), XRD, CO chemisorption measurements, and field-emission transmission electron microscopy (FE-TEM). The silanol group (–OH), which is one of the functional groups of SiO_2, interferes with the reduction of palladium because it strongly bonds with palladium ions (–PdO) during the preparation of the catalyst. Due to the complete removal of silanol (Si–OH) groups following calcination at 700 °C, the metal reducibility was enhanced, and the catalyst pretreated at this calcination temperature exhibited the highest metal dispersion of 13.02%. Further, to confirm the catalytic activity of the prepared catalysts, hydrogenation of D-glucose was conducted. The HPLC results demonstrated that Pd/SiO_2_700 has the highest catalytic activity toward hydrogenation of D-glucose. Therefore, it was confirmed that the removal of silanol groups increase the metal dispersion and catalytic activity of Pd/SiO_2 catalyst.

Keywords: Hydrogenation, Metal Dispersion, Palladium Catalyst, Thermal Treatment.

1. INTRODUCTION

Various types of catalysts are widely employed in industries for processes such as hydrogenation, dehydrogenation, and petroleum cracking. Particularly, metal oxides and noble metal catalysts (i.e., catalysts containing Pd, Pt, Rh, Ag, and Au, among others) are commonly used because of their favorable reaction rates and reaction selectivities. However, noble metals are expensive and finite resources, and tend to undergo sintering at high temperatures. Therefore, deposition of noble metals on supports with large surface areas and high stabilities is required.[1] The support greatly influences the catalytic performance of a system, as it can change the charge and size of the metal particles, in addition to forming active sites at the metal-support boundaries.[1,2] The catalytic activities of noble metals are strongly influenced by the surface properties of supports, as changes in the metal-support interactions can result in metal dispersion and affect the reducibility of the supported metal.[3]

Silica (SiO_2) is one of the most extensively used catalyst supports due to its high surface area, ample porosity, good stability, and morphological stability at high temperatures. In addition, it is inert and does not participate in the catalytic reaction.[2,4] However, SiO_2 is an irreducible oxide and exhibits weak metal-support interactions compared to other metal oxides.[4–6] These properties render the deposition of noble metals on the support surface particularly challenging. Therefore, modification of the SiO_2 surface is required to increase the catalyst preparation efficiency.

To date, a number of support pretreatment methods have been reported, including calcination[2] and pretreatment with nC1–C5,[7] organic solvents,[3] and ammonia.[8] Such pretreatment controls the chemical properties of the SiO_2 surface, including the functional groups present on the support. SiO_2 contains a range of functional groups that are formed during its preparation;[4,6,9] for example, silanol groups present on the surface can suppress the reduction of the noble metal precursor, thereby decreasing metal dispersion, which is an important factor for determining catalytic activity.[7,8,10] As the silanol groups can

*Author to whom correspondence should be addressed.

1533-4880/2019/19/882/006 doi:10.1166/jnn.2019.15943

contribute to strong interactions between the metal species and oxygen on the SiO_2 support, metal reducibility can decrease through such interactions.

The activities of the prepared catalysts were confirmed by hydrogenation of D-glucose into D-sorbitol. D-sorbitol is a sugar alcohol that is widely used in food industry, cosmetics, and medical industries.[11] Furthermore, sorbitol is applied as a starting material for vitamin C synthesis, ethylene glycol, and glycerol.[12, 13] Although the conversion of D-glucose to D-sorbitol appears simple, in reality, a side reaction can occur instead of conversion into sorbitol. For example, D-glucose can be isomerized to D-fructose by the Lobry de Bruyn-Alberdavan Ekenstein reaction.[14] Thus, Pd having a high affinity toward hydrogen is suitable as a catalyst for D-glucose hydrogenation without glucose-fructose isomerization.

In this study, we report the modification of SiO_2 by calcination at a range of temperatures between 300 and 1100 °C to examine the effect of surface silanol concentration on the SiO_2 support on the physico-chemical properties of SiO_2-supported Pd catalysts. In addition, hydrogenation of D-glucose into D-sorbitol was conducted to gain further understanding of the role of Pd dispersion in D-glucose hydrogenation. Combining the best results from the hydrolysis and hydrogenation steps will enable confirming the effect of metal dispersion on hydrogenation.

2. EXPERIMENTAL DETAILS

2.1. Materials

Silicon dioxide (SiO_2, 99.5%, Sigma Aldrich) was employed as the support, and sodium tartrate ($Na_2C_4H_4O_6$, ≥99%, Sigma Aldrich), hydrochloric acid (HCl, 38%, Dae Jung), palladium chloride ($PdCl_2$, ≥99%, Sigma Aldrich), sodium borohydride ($NaBH_4$, 95%, Sigma Aldrich), and sodium hydroxide (NaOH, ≥98%, Sigma Aldrich) were used during catalyst preparation. In addition, D-glucose ($C_6H_{12}O_6$, ≥99.5%, Sigma Aldrich) was used for hydrogenation. Standard materials such as analytical reagent-grade D-sorbitol ($C_6H_{14}O_6$, ≥98%), fructose ($C_6H_{12}O_6$, ≥99%), and glycerol ($C_3H_{12}O_3$, ≥99%) were purchased from Sigma-Aldrich. Nitrogen and hydrogen gases with a minimum state purity of 99.0% were obtained from GASTEC KOREA.

2.2. Catalyst Preparation

Pd/SiO_2 catalysts were prepared using an ion-exchange method. Initially, SiO_2 supports were calcined at desired temperatures between 300 and 1100 °C, and the obtained supports were labelled as SiO_2_100, SiO_2_300, SiO_2_500, SiO_2_700, SiO_2_900, and SiO_2_1100, where the number indicates the calcination temperature. A 0.1 M solution of $PdCl_2$ in HCl was employed as the metal precursor, and a portion of this solution was added to a 1 mM solution of sodium tartrate at 5 °C. A desired quantity of pretreated SiO_2 was then dispersed into this solution and the solution pH was adjusted to 6.0 by adding an aqueous NaOH solution. After stirring for 2 h, a freshly prepared 0.3 M solution of sodium borohydride was added to the above solution and stirred at 5 °C for 2 h to reduce the Pd salts to Pd metal particles. The catalysts were then isolated by filtration and washed with distilled water until a pH of 5–6 was reached. Finally, the catalysts were dried at 110 °C for 12 h.

2.3. Characterization

The specific surface areas and porous structures of the pretreated supports were examined by nitrogen physisorption (ASAP2020 Surface Area Analyzer, USA) at −196 °C. The samples were degassed under vacuum at 150 °C for 4 h prior to measurement. The silanol group concentration was obtained by Fourier transform infrared spectroscopy (FT-IR, Nicolet 6700, Thermo Fisher, USA) and ammonia temperature-programmed desorption measurements (NH_3-TPD, AutoChem 2920, Micromeritics Instruments Corp., USA). X-ray diffraction (XRD, D/MAX 2500 V PC, Rigaku, Japan) was used to characterize the crystal structures of the pretreated supports and the prepared catalysts in the 2θ range of 10–90°, and field-emission transmission electron microscopy (FE-TEM, JSM-6700F, JEOL, Japan) was used to determine the particle sizes and distributions of the deposited Pd. H_2 uptake during the reduction process was measured by temperature-programmed reduction with hydrogen (H_2-TPR, AutoChem 2920, Micromeritics Instruments Corp., USA), while the Pd dispersions were evaluated by examining the CO adsorption capacity using a pulse technique (CO-chemisorption, AutoChem 2920, Micromeritics Instruments Corp., USA) assuming a Pd:CO adsorption ratio of 2:1.

2.4. Hydrogenation of D-Glucose

The reaction was performed in batches in a 100-mL stainless steel autoclave. The hydrogenation reaction was performed by charging the autoclave with 60 mL of glucose solution (10 g/L) and 150 mg of the prepared catalysts with different Pd dispersions. All the catalytic tests were performed at 120 °C and 2.5 MPa of pure hydrogen for 360 min.[15] The reactor was purged with N_2. Thereafter, hydrogen was introduced to purge out nitrogen to 1.0 MPa. After setting the reaction temperature, the pressure was raised to 2.5 MPa. The product distribution was analyzed by HPLC (Agilent, HPLC sereies1200) equipped with a RI detector and Hi-Plex Ca (300∗7.7 mm) column and operated at 80 °C with an eluent water flow rate of 0.5 mL/min. D-glucose conversion, D-sorbitol yield, and selectivity were calculated using Eqs. (1)–(3).[13]

$$X_{\text{D-gluose}}\ (\%) = \frac{\text{mole(D-Glucose}_0) - \text{mole(D-Glucose}_f)}{\text{mole(D-Glucose}_0)} \times 100 \quad (1)$$

$$S_{\text{Sorbitol}}\ (\%) = \frac{\text{mole(Sorbitol)}}{\text{mole(D-Glucose}_0) - \text{mole(D-Glucose}_f)} \times 100 \quad (2)$$

$$Y_{\text{Sorbitol}}\ (\%) = \frac{\text{mole(Sorbitol)}}{\text{mole(D-Glucose}_0)} \times 100 = \frac{X \times S}{100} \quad (3)$$

3. RESULTS AND DISCUSSION

3.1. Characterization of Pretreated SiO_2 Support

Table I shows the characteristics of the SiO_2 supports calcined at different calcination temperatures. As indicated, the specific surface area of the support decreased only slightly with increase in calcination temperature from 300 to 700 °C, while a dramatic reduction was observed at higher temperatures. This is possibly due to the aggregation and sintering of SiO_2 particles above 900 °C.[8] In addition, SiO_2_1100 exhibited a particularly low specific surface area of 0.42 m^2/g due to phase transition from amorphous to cristobalite phase.[16]

The XRD profiles of the calcined SiO_2 supports are shown in Figure 1. As indicated, amorphous SiO_2 was abundant following calcination ≤900 °C. However, after calcination at 1100 °C, peaks corresponding to cristobalite were observed at $2\theta = 21.92$, 28.38, 31.38, 36.1, 48.52, and 57.06° due to an increase in the crystallinity of SiO_2 and corresponding phrase transition at high temperatures.[17]

In addition to specific surface area and the silica phase, silanol group concentration on the SiO_2 surface also plays an important role in the dispersion of metal particles on SiO_2.[18, 19] To examine the effect of calcination temperature on the silanol groups, FT-IR and NH_3-TPD were employed. As shown in the FT-IR spectra (Fig. 2), Si–O–Si stretching and bending vibrations were observed at 1150, 780, and 480 cm^{-1} in addition to a silanol stretching vibration at 960 cm^{-1}.[3, 8] Comparison with untreated silica support (SiO_2_100) revealed that high calcination temperatures resulted in decreased quantities of silanol groups, with complete removal observed at temperatures ≥700 °C.[8]

This was also confirmed by NH_3-TPD measurements, as outlined in Table II, which shows the strengths of acidic sites (i.e., silanol groups) on various calcined supports.[20] In principle, both the concentration of sites having similar acid strengths and the average adsorption heat or activation energy of NH_3 desorption can be determined using the TPD method. The appearance of the TPD peak is associated with the presence of strongly acidic hydroxyls as sorption sites.[21] As indicated, an increase in calcination temperature resulted in a decrease in ammonia adsorption peak areas of the supports, with a sharp drop observed at temperatures ≥700 °C. Moreover, phase transition following calcination at 1100 °C resulted in almost complete removal of the silanol groups.

Table I. Textural properties of SiO_2 supports with different calcination temperature.

Supports	Specific surface area (m^2/g)	Pore volume (cm^3/g)	Pore size (nm)
SiO_2_100	172.62	1.122	38.05
SiO_2_300	150.23	0.663	16.09
SiO_2_500	132.07	0.699	25.29
SiO_2_700	119.58	0.517	22.49
SiO_2_900	51.33	0.190	23.73
SiO_2_1100	0.42	0.0011	10.956

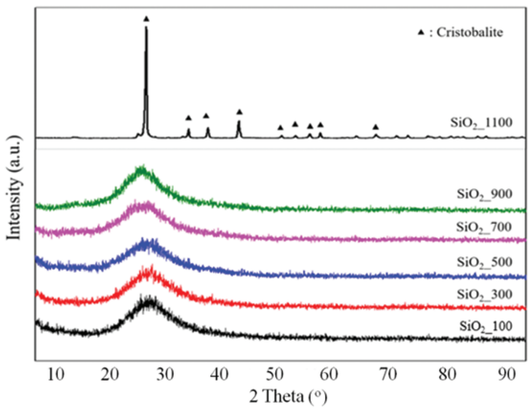

Figure 1. XRD patterns of pretreated SiO_2 supports.

3.2. Catalyst Characterization

The specific surface areas and pore properties of the various catalysts are summarized in Table III, where slight decreases in specific surface areas and pore volumes of the Pd-modified catalysts are observed as compared to those of the bare supports.[22]

The XRD patterns of the prepared catalysts are presented in Figure 3, where a broad diffraction peak at 22.21° (corresponding to amorphous silica) is apparent for all the supports calcined at temperatures ≤900 °C.

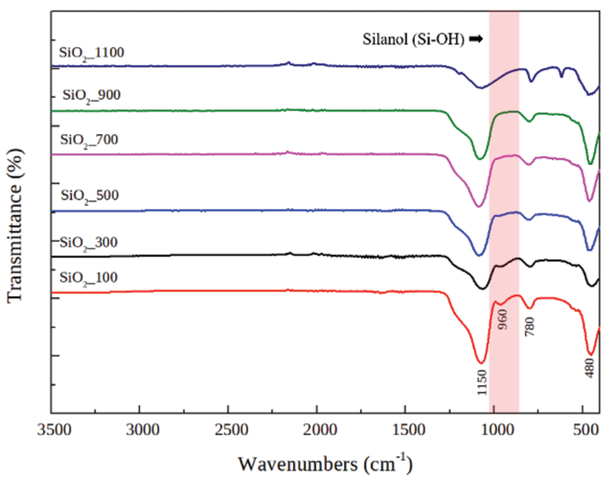

Figure 2. FT-IR spectra of pretreated SiO_2 supports.

Table II. NH_3-TPD peak areas of calcined SiO_2.

Supports	Total acidic sites (mmol/g)[a]
SiO_2_100	1.167
SiO_2_300	0.728
SiO_2_500	0.575
SiO_2_700	0.248
SiO_2_900	0.271
SiO_2_1100	0.099

Note: [a]Based on NH_3-TPD measurements.

In addition, strong diffraction peaks at 40.1, 46.9, 68, and 82.1° were observed for all the catalysts, possibly due to the presence of crystalline Pd. In addition, compared to the Pd peaks of the Pd/SiO_2_100 catalyst, the calcined supports exhibited significantly broader Pd signals, with Pd/SiO_2_700 showing the broadest Pd peak. These results suggest that Pd particles on the SiO_2_700 support are dispersed evenly, as the broad signals are associated with small Pd crystallite sizes.[23] These results correspond closely with the CO chemisorption results.

H_2-TPR experiments were then performed (Fig. 4) to study the effect of thermal and chemical aging on the reducibility of Pd species and to understand the role of silanol groups in metal-support interactions. As shown in Figure 4, an H_2 uptake peak is present between 50 and 80 °C for all the samples.[24] However, with increase in calcination temperature to 700 °C, the intensity and area of the signal decreased, and the H_2 uptake peak shifted to lower temperatures. With further increase in calcination temperature above 900 °C, the signal intensity and area increased once again and the peak shifted to higher temperatures. These results suggest that the Pd species of Pd/SiO_2_700 can be most easily reduced compared to that of the various catalysts examined herein.[25] In addition, upon increasing the calcination temperature, strained and weakened siloxane bridges (≡Si–O–Si≡) are formed on the hydroxylated SiO_2 surface. At higher temperatures and without vicinal OH groups on the surface, the strained siloxane groups are converted into stable siloxane bridges and rings.[6] Removal of the silanol groups thereby decreases the metal reducibility, while the formation of stable siloxane groups leads to aggregation of the Pd particles. From these results, it is apparent that calcination of the support at 700 °C is the optimal pretreatment temperature for the preparation of highly dispersed Pd/SiO_2 catalysts.

Table III. Textural properties of Pd/SiO_2 catalysts with different calcination temperature.

Catalysts	Specific surface area (m^2/g)	Pore volume (cm^3/g)	Pore size (nm)
Pd/SiO_2_100	153.25	0.576	19.35
Pd/SiO_2_300	148.97	0.534	20.67
Pd/SiO_2_500	114.36	0.495	21.65
Pd/SiO_2_700	103.776	0.462	22.421
Pd/SiO_2_900	50.340	0.133	15.395
Pd/SiO_2_1100	0.024	0.0015	240.99

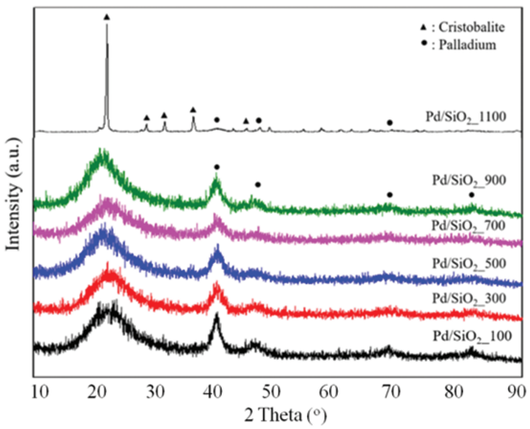

Figure 3. XRD patterns of prepared Pd/SiO_2 catalysts.

Table IV shows the Pd dispersion percentages as determined by CO chemisorption measurements and calculation of the CO uptake. As indicated, metal dispersion increased with increasing calcination temperature up to 700 °C, with Pd/SiO_2_700 exhibiting the highest Pd dispersion of 13.02%. The combination of these results with those of FT-IR and N_2 physisorption measurements suggests that a decline in the number of silanol groups leads to an increase in metal dispersion, as the silanol groups resulted in strong interactions between Pd and oxygen, thereby inhibiting the reduction of Pd. During the preparation of Pd/SiO_2, the

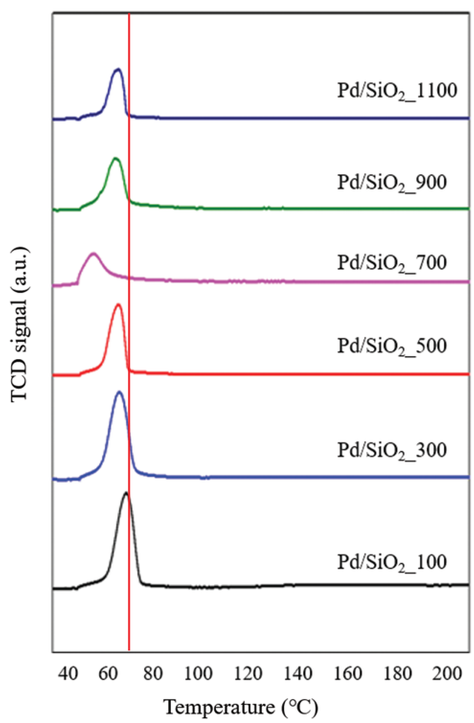

Figure 4. H_2-TPR profiles of the Pd/SiO_2 catalysts.

Table IV. CO-chemisorption of prepared Pd/SiO_2 catalysts.

Catalysts	Metal dispersion (%)	Cumulative quantity (mmol/g)	Metallic surface area (m^2/g)
Pd/SiO_2_100	2.90	0.007	12.93
Pd/SiO_2_300	5.07	0.012	22.60
Pd/SiO_2_500	6.18	0.015	27.51
Pd/SiO_2_700	13.02	0.024	44.81
Pd/SiO_2_900	7.97	0.019	35.52
Pd/SiO_2_1100	5.61	0.013	24.99

following reactions occurred:

$$\text{surface-SiOH} \overset{K_1}{\longleftrightarrow} \text{surface-SiO}^- + \text{H}^+ \quad (4)$$

$$\text{surface-SiO}^- \overset{K_2}{\longleftrightarrow} \text{surface-SiOPd}^+ \quad (5)$$

$$K_1 = \frac{[\text{surface-SiO}^-][\text{H}^+]}{[\text{Surface-SiOH}]} \quad (6)$$

$$K_2 = \frac{[\text{surface-SiOPd}^+]}{[\text{Pd}^{2+}][\text{Surface-SiO}^-]} \quad (7)$$

Van Steen et al.[26] suggested that surface-$SiOPd^+$is the precursor of strongly interacting metal species.

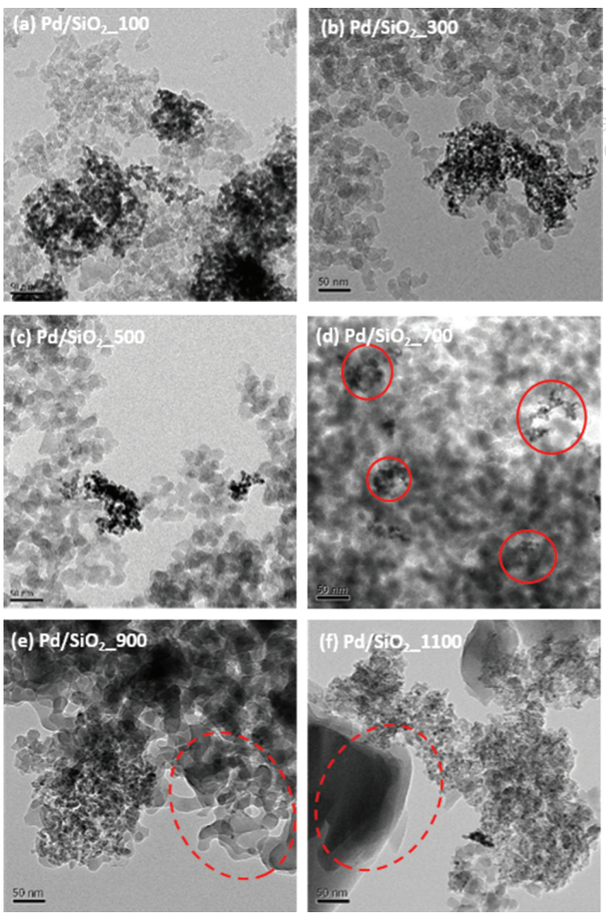

Figure 5. FE-TEM images of prepared Pd/SiO_2 catalysts.

Substitution of Eq. (6) into Eq. (7) gives:

$$[\text{surface-SiOPd}^+] = K_2[\text{Pd}^{2+}][\text{surface-SiO}^-] = \frac{K_2K_1[\text{surface-SiOH}][\text{Pd}^{2+}]}{[\text{H}^+]} \quad (8)$$

The concentration of surface-$SiOPd^+$ is only proportional to the surface concentration of silanol when the Pd salts were fixed. Thus, the higher the silanol concentration, the stronger is the interaction between metal and SiO_2, which will result in low palladium reducibility;[3] that is, the removal of silanol groups enhances metal reducibility.[7, 8, 23] However, the metal dispersions of Pd/SiO_2_900 and Pd/SiO_2_1100 decreased to 7.97 and 5.61% despite the absence of silanol groups, thereby suggesting dramatic decreases in the specific surface areas and pore volumes of SiO_2 following calcination above 900 °C.[2]

Figure 5 shows the Pd particle sizes and distribution of Pd as visualized by FE-TEM. These images confirm an average Pd particle size of ~5–10 nm. In addition, the supported Pd particles became evenly dispersed upon increasing the support calcination temperature up to 700 °C, while above 900 °C, condensation of the SiO_2 particles resulted in sintering.

These results support the observations that the removal of silanol groups affects the dispersion of Pd, and that aggregation negatively affects Pd dispersion.[2] It is therefore apparent that calcination of SiO_2 at an appropriate temperature can improve the dispersion of Pd particles on the support surface.

3.3. Hydrogenation of D-Glucose

The catalytic activities of the prepared Pd/SiO_2 catalysts for the hydrogenation of D-glucose were investigated. The effect of palladium dispersion on the hydrogenation of D-glucose was shown in Figure 6 and Table V. The yield

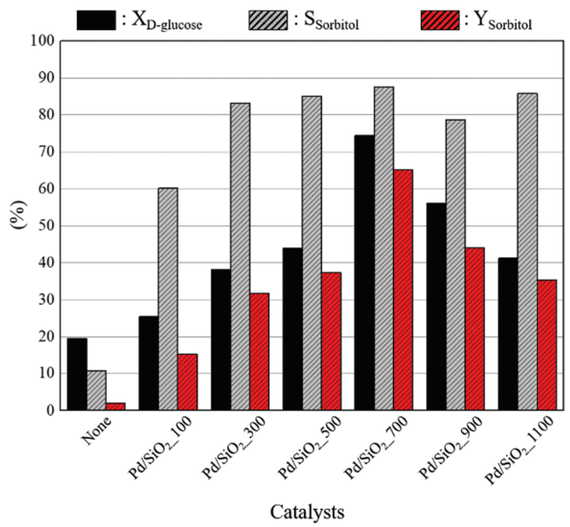

Figure 6. Diagram of D-glucose hydrogenation.

Table V. Effect of Pd dispersion on hydrogenation.

Catalysts	Conversion (%)	Selectivity (%)	Yield (%)
None	19.47	10.72	2.09
Pd/SiO_2_100	25.41	60.14	15.29
Pd/SiO_2_300	38.17	83.14	31.73
Pd/SiO_2_500	43.92	85.01	37.33
Pd/SiO_2_700	74.35	87.56	65.11
Pd/SiO_2_900	56.05	78.62	44.07
Pd/SiO_2_1100	41.24	85.74	35.36

of sorbitol increased with increase in Pd metal dispersion in the order: Pd/SiO_2_700 (65.11%) > Pd/SiO_2_900 (44.07%) > Pd/SiO_2_500 (37.34%) Pd/SiO_2_1100 (35.36%) > Pd/SiO_2_300 (31.73%) > Pd/SiO_2_100 (15.29%). Sorbitol was hardly produced in the absence of a catalyst with only 2.09% yield. When hydrogenation reaction was carried out using Pd/SiO_2_700 that has the highest metal dispersion, a high yield of 65.10% was obtained.

These indicate that the highest yield (using Pd/SiO_2_700) was more than about 4 times the yield of the catalytic reaction with Pd/SiO_2_100. It is confirmed that the results are related to metal dispersion on hydrogenation of D-glucose since the catalyst with high Pd dispersion collides more efficiently with the reactant compared to the catalyst with low Pd dispersion. These results indicate that the catalyst with high metal dispersion has increased catalytic activity.

4. CONCLUSION

We herein presented our results on the effects of variation in support (SiO_2) calcination temperature on the preparation and properties of Pd/SiO_2 catalysts. As the calcination of SiO_2 can lead to a decrease in the number of silanol groups on the support surface, the reduction of Pd is inhibited and a low metal dispersion is observed, as the silanol groups promote strong interactions between Pd and SiO_2. Indeed, at calcination temperatures >700 °C, the silanol groups were completely removed. At temperatures up to 700 °C, an increase in Pd dispersion was observed, with the highest dispersion of 13.02% achieved for the Pd/SiO_2_700 catalyst. However, upon increasing the calcination temperature above 900 °C, a dramatic decrease in specific surface area was observed, accompanied by a decrease in Pd dispersion to 5.61%.

The catalytic activity was examined by conducting hydrogenation of D-glucose using the prepared catalysts with different metal dispersions, and the effect of Pd dispersion on catalytic activity was confirmed. Experimental results showed that hydrogenation with Pd/SiO_2_700 having the highest dispersion (13.02%) resulted in a much higher sorbitol yield of 65.10% compared to other catalysts. It was confirmed that as the palladium particles are evenly distributed, the number of effective collisions between the reactant and the catalytic active sites increases, and thus, the catalytic activity increases with the use of highly dispersed catalyst.

These results represent the development of a simple method for the modification of surface properties of catalyst supports, which will ultimately lead to enhanced catalytic activities.

Acknowledgment: This research was financially supported by a Private Finance Research Project (Project No. IR170027) and by the Korea Institute of Industrial Technology (KITECH) (Project No. JA180001).

References and Notes

1. J. S. Kim, J. H. Baek, M. H. Kim, S. S. Hong, and M. S. Lee, *Mater. Sci. Forum* 804, 149 (**2014**).
2. Z. Qu, W. Huang, S. Zhou, H. Zheng, X. Liu, M. Cheng, and X. Bao, *J. Catal.* 234, 33 (**2005**).
3. S. H. I. Lihong, L. I. Debao, H. O. U. Bo, and S. U. N. Yuhan, *Chinese Jounal of Catalyiss* 28, 999 (**2007**).
4. B. K. Min, A. K. Santra, and D. W. Goodman, *Catal. Today* 85, 113 (**2003**).
5. M. Jacquemin, D. Hauwaert, D. P. Debecker, and E. M. Gaigneaux, *J. Mol. Catal. A Chem.* 416, 47 (**2016**).
6. L. T. Zhuravlev, *Colloids Surfaces A Physicochem. Eng. Asp.* 173, 1 (**2000**).
7. D. Jiang, Y. Ding, Z. Pan, W. Chen, and H. Luo, *Catal. Letters* 121, 241 (**2008**).
8. R. Lu, D. Mao, J. Yu, and Q. Guo, *J. Ind. Eng. Chem.* 25, 338 (**2015**).
9. P. K. Jal, S. Patel, and B. K. Mishra, *Talanta* 62, 1005 (**2004**).
10. J. Yang, B. Li, H. Xu, Y. Li, and X. Huo, *J. Fiber Bioeng. Informatics* 7, 117 (**2014**).
11. K. Van Gorp, E. Boerman, C. V. Cavenaghi, and P. H. Berben, *Catal. Today* 52, 349 (**1999**).
12. T. W. Pacific, N. National, G. P. National, and R. Energy, 1, 58 (**2004**).
13. A. Romero, E. Alonso, and A. Nietom, *Microporous Mesoporous Mater.* 224, 1 (**2016**).
14. D. Kumar, A. Asharaf, J. Je, S. Hwa, and J. Hwang, *Catal. Today* 232, 99 (**2014**).
15. L. M. Sanz-Moral, A. Romero, F. Holz, M. Rueda, A. Navarrete, and A. Martín, *J. Taiwan Inst. Chem. Eng.* 65, 515 (**2016**).
16. A. Palermo, J. P. Holgado Vazquez, A. F. Lee, M. S. Tikhov, and R. M. Lambert, *J. Catal.* 177, 259 (**1998**).
17. Y. Arai, Y. Aoki, and Y. Kagawa, *Scr. Mater.* 139, 58 (**2017**).
18. R. K. Iler, *Chem. Silica* 622, 372 (**1979**).
19. C. Brinker and G. Scherer, Sol-Gel Science: The Physics and Chemistry of Sol-Gel Processing, Academic Press, New York (**1990**), pp. 618–668.
20. S. X. Wang, R. T. Guo, W. G. Pan, Q. L. Chen, P. Sun, M. Y. Li, and S. M. Liu, *Catal. Commun.* 89, 143 (**2017**).
21. J. V. F. Lónyi, *Microporous Mesoporous Mater.* 47, 293 (**2001**).
22. J. S. Kim, S. Hong, J. Kim, and M. S. Lee, *Appl. Chem. Eng.* 26, 575 (**2015**).
23. V. V. Dutov, G. V. Mamontov, V. I. Zaikovskii, and O. V. Vodyankina, *Catal. Today* 278, 150 (**2016**).
24. S. K. Matam, E. H. Otal, M. H. Aguirre, A. Winkler, A. Ulrich, D. Rentsch, A. Weidenkaff, and D. Ferri, *Catal. Today* 184, 237 (**2012**).
25. M. F. Luo, Z. Y. Hou, X. X. Yuan, and X. M. Zheng, *Catal. Letters* 50, 205 (**1998**).
26. E. Van Steen, G. S. Sewell, R. A. Makhothe, C. Micklethwaite, H. Manstein, M. De Lange, and C. T. O. Connor, 229, 220 (**1996**).

Received: 1 November 2017. Accepted: 31 March 2018.